



Monitoring the Environmental Risks Around Medinet Habu and Ramesseum Temple at West Luxor, Egypt, Using Remote Sensing and GIS Techniques

Abdelaziz Elfadaly^{1,2,3} · Wael Attia³ ·
Rosa Lasaponara²

Published online: 2 August 2017

© Springer Science+Business Media, LLC 2017

Abstract Today, the preservation of cultural heritage is a pressing issue especially for territories subjected to a long period of human action that could adversely influence environment and heritage properties, thus producing a deterioration of archaeological features and alteration of historical landscape. In this paper, the environmental risks and their effects on preservation issues are investigated for the archaeological area of the Luxor city (south of Egypt) where the most famous Temples in Egypt are located. A comprehensive analysis has been conducted for the Ramesseum and Medinet Habu temples considering their building material and characteristics, environmental (geological and hydrological) setting, and past and ongoing changes around the monument areas. Satellite multitemporal images have been used to detect all the changes mainly linked to the expansion of urban and agriculture areas. Results from the analysis conducted along with *in situ* investigations have suggested that many of the environmental problems around the archaeological areas are coming as a result of urban and agriculture sprawling. Both of them strongly influence the distribution in the levels of groundwater which along with temperature are considered as the main causes of the deterioration process affecting the Medinet Habu and Ramesseum temple. The degree of weathering damage appears to be much more dependent on exposure characteristics of

✉ Rosa Lasaponara
rosa.lasaponara@imaa.cnr.it

Abdelaziz Elfadaly
Abdelaziz.elfadaly@unibas.it

Wael Attia
wael.gis@gmail.com

¹ UNIBAS, University of Basilicata, Potenza 85100, Italy

² CNR-IMAA, C.da S. Loja 85050 Tito Scalco (PZ), Potenza, Italy

³ NARSS, National Authority for Remote Sensing & Space Sciences, Cairo, Egypt

the investigation areas, especially as related to salt weathering processes. Innovative solutions to support the preservation of these temples are herein presented and discussed.

Keywords Environmental risks · Medinet Habu · Ramesseum · Luxor · Remote sensing · GIS

Introduction

The preservation and enhancement of cultural heritage is today one of strategic priorities not only to assure cultural treasures to future generations but also to exploit them as a strategic economic asset inspired to sustainable development strategies. This is an extremely important key factor for the countries, as Egypt, which are owners of an extraordinary cultural legacy, which must be preserved from alterations induced by natural decay and/or accelerated by anthropogenic activities.

Today, as also highlighted by UNESCO, cultural heritage is “increasingly threatened with destruction not only by the traditional causes of decay, but also by changing social and economic conditions which aggravate the situation with even more formidable phenomena of damage or destruction” (from the general conference of the United Nations Educational, Scientific and Cultural Organization meeting in Paris from 17 October to 21 November 1972, at its 17th session, available online (<http://whc.unesco.org/en/conventioncontext/>)). According to UNESCO, the factors that most of all threaten cultural heritage sites are urban sprawl, pollution, biological resource use/modification, physical resource extraction, local conditions affecting physical fabric, social/cultural uses of heritage, climate change, severe weather events, sudden ecological or geological events, management and institutional factors, transportation and utilities infrastructure, invasive/alien or hyperabundant species, the deliberate destruction, terrorism, or civil unrest.

In this context, as also suggested by UNESCO, it is important to highlight that cultural heritage and landscape especially where heavily influenced by human activities have to be systematically monitored and managed accordingly to be preserved. Systematic monitoring activities may provide effective information and tools for assessing threats and risks on historical buildings, landscape, and buried remains. Satellite remote sensing can provide useful information for setting up of *ad hoc* plan to support systematic monitoring, preservation activities, and mitigation strategies for the survival of cultural properties including archaeological heritage and landscape.

According to several authors (Levin 1999; Skidmore 2003; Johnson 2006; Wiseman and El-Baz 2007; Kelong *et al.* 2008; Parcak 2009; Khorram *et al.* 2012; Butt *et al.* 2015; Mosbeh and Kaloop 2015), remote sensing and historical archives can be fruitfully used as a baseline dataset in documenting and analyzing both historical and contemporary effects of human activities on cultural heritage sites.

An integrated approach based on remote sensing (RS) and geographic information system (GIS) allows cultural resource managers, historians, planners, and engineers to catalog and assess the organizational and structural patterns of such sites, and determine sustainable tourism and urban development within their regions. Early remote sensing applications in archaeology started in the 1920s (Orlando and Villa 2011). Since this date, aerial photography has been used in archaeology primarily to view features on the

earth's surface, which are difficult if impossible to visualize from the ground level (Alexakis *et al.* 2012). Remote sensing technique is today employed as operational tool in detecting surface and underground archaeological remains (see, for example, Lasaponara *et al.* 2016; Tapete *et al.* 2013; Lasaponara and Masini 2013a, b; Masini *et al.* 2009; Lasaponara *et al.* 2011; Masini and Lasaponara 2006) as well for the documentation, monitoring, and preservation of cultural heritage (Cigna *et al.* 2014).

From the mid-1970s, satellite remote sensing has played an increasing role in elucidating both the cultural and environmental development of alluvial landscapes (Challis and Andy Howard 2006), while modern digital spectral sensors were first used for archaeological prospection in the late 1980s (Bennett 2011). There are many advantages to conducting a remote sensing survey when compared to a ground campaign (Corrie 2011). The use of multispectral satellite images of medium resolution (Landsat TM/ETM+, and ASTER) and high resolution (QuickBird, IKONOS, and GeoEye) provide further perspectives of remote sensing techniques, beyond the visible spectrum, for the detection of buried remains (Agapiou *et al.* 2011). The archaeological community has also recently seen the need for near-surface mapping using GPR in order to identify buried cultural remains for protection and future preservation and as a planning tool for selective excavation, as regards remote sensors and space segment, the space shuttle provides a unique opportunity to test variety of sensors-shuttle imaging radar (sin), multispectral optoelectronic modular scanner (MOMS), metric camera, microwave remote sensing experiment (MRSE), *etc.* (Rajan and Ninan 1983). The most immediate applications of remote sensing technology and image processing should be in the analysis of the environments of human societies and their interrelationships thereby generating and testing models both of human behavior and of environmental change (Roudgarmi *et al.* 2008; Lasaponara and Masini 2012).

In this paper, the environmental risks and their effects on preservation issues are investigated for the archaeological area of the Luxor city (south of Egypt) where the most famous Temples in Egypt are located. Ramesseum temple and Medinet Habu are two of these temples located at the west side of the Luxor city. The Ramesseum temple, which was built for Ramesses II, was begun before the end of the second year of his reign. The decoration of the monument was undertaken not before the fifth year and probably ended in year 1213 BC. While the Ramesseum was built by a more famous pharaoh (Ramesses II), Medinet Habu, commissioned by Ramesses III, is a much more impressive sight with its pylon and many of its walls still intact and much more of the original painting visible on its carved surfaces. Ramesses III (reign 1184–1153 BC) was the last of the great pharaohs of Egypt. During his reign, Medinet Habu functioned as a walled city with the temple and an administrative center inside of walls that protected the inhabitants of the area during hard times. Later on, the complex became a walled town for Coptic Christians living in the area. Unfortunately, most of these Temples are suffering from a bad environmental status, additional to the continually increasing population. Many of the environmental problems around the archaeological areas come as a result of urban and agriculture sprawling. In this paper, a comprehensive analysis has been conducted considering archaeological and environmental (geological and hydrological) features as well as past and ongoing changes around the monument areas assessed using satellite data.

The integrated analysis was conducted into a GIS environment in order to (i) integrate results from archaeological, geological, and hydrological studies and remote sensing and (ii) facilitate the interpretation of the results. Outputs from our investigations highlighted that the degree of weathering damage appears to be much more dependent on exposure characteristics of the investigation areas and the local environmental conditions, especially as related to salt weathering processes. Finally, on the basis of the outputs of our analysis, innovative solutions are suggested to contribute to the preservation and systematic monitoring of this invaluable archaeological area.

Study Area and Environmental Setting

Study Area

The ancient Theban necropolis is located 600 km (DMS long. $32^{\circ} 38' 22.6932''$ E, DMS lat. $25^{\circ} 41' 14.0748''$ N) south of Cairo on the west bank of the River Nile (McLane *et al.* 2003). On the Nile's west bank, across from Luxor, is Thebes, the capital of Egypt from around 2000 to 1075 BCE (Middle and New Kingdoms). Thebes became a burial ground for kings, queens, priest, and nobles. Also buried here are priests, nobles, royal children, and tomb builders (Dliffc 2011) (Fig. 1).

- Ramesseum Temple

The “Ramesseum”—the great temple built by Ramesses II, where future ages should worship him—is one of the most impressive ruins of Thebes (Quibell 1898), located at Sheikh Abd el-Qurna, almost 2 km to the southwest of Sety's mortuary temple. Enclosing an area of $210\text{ m} \times 178\text{ m}$, Ramesses's mortuary temple was much more grandiose than that of his father (Fig. 2).

The description of the Ramesseum temple, given by Diodorus, is so accurate that it is obvious he was writing from personal knowledge: “The sepulcher of Simandius

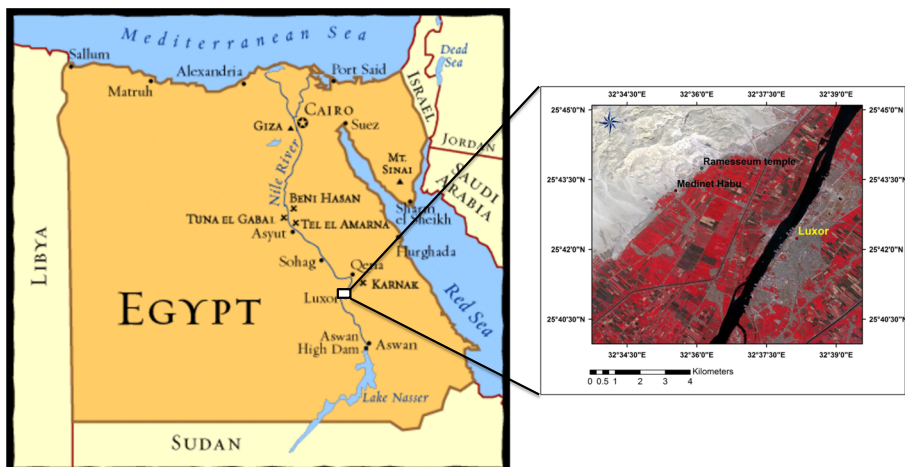


Fig. 1 Map of Egypt and study area by “Spot5 satellite image” 2015 (RGB composite)



Fig. 2 Hypostyle hall and the surrounded mudbrick rooms of Ramesseum temple

contained above half a league about, at the entrance whereof was a great of porphyry, next to which was a square gallery of stone, in to on the tops of the pillars were architraves all of one stone, and the covering was all of stone, ten foot broad, enriched with azure stars” (Murray 2002). A pylon of Ramesseum admits to a court with a colonnade on the north and south sides, that on the south forming the facade of Ramesses’ palace, which was built along this side of the temple. The inner face of the first pylon and the upper part of the walls behind the colonnades in the northern half of the second court are devoted to a representation of the great harvest festival, yearly celebrated in honor of Min and apparently also in commemoration of the Pharaoh’s accession (Blackman 1923). Upon the completion of the walls, mudbrick buildings were roofed in one of two fashions: with flat roofs or with vaulted roofs (Virginia 2011).

– Medinet Habu

The great temple, once the nucleus of the entire building project of Ramesses III, remains today the center and the predominant feature of Medinet Habu, as, except for the small temple and a few chapels of the later periods, it is the only building still comparatively fully preserved among the surrounding ruins (Holscher 1941). The palace of Habu is full 2000 ft square. The peristyle court is the most stupendous, and appears calculated for the grand audience court of the Pharaohs (Bednarski 2005). The final version of the architectural plan, allowed for the expansion of the repository to twice its size— 10×20 cwt—presumably to permit the visits of a larger portable conveyance, omitted the planned transverse hall, inadvertently resulting in insufficient foundational support for the western wall of the enlarged repository, which was to create, in time, structural problems in this portion of the temple (Fisher 2009) (Fig. 3).

Medinet Habu inscriptions, which discuss how he protected Egypt’s northern border from waves of external invasion, represent one of his presentations of power. While his claims should not be taken literally, the inscriptions have value by ideological messages that served to strengthen his authority (Peters 2011).



Fig. 3 The complex of Medinet Habu

Geological Setting

The city of Luxor is geologically part of the Stable Shelf characterized by alluvium deposits at the sides of the river Nile, and surrounded by Oligocene, Eocene, and Miocene areas covered by sand deposits. Underneath the Memnon Colossi (neighbor to Habu and Ramesseum) are silt layers of low shear strength, about 6 m in thickness, resting on a compacted limestone of the Shelf (Casciati and Borja 2004). The Pliocene unit comprises the sediments of the Paleonile river system. It is represented in Luxor area by two formations, namely, Pliocene fault breccia or intraformational conglomerate and Medamud. The recent alluvial cover comprises unconsolidated sediments,

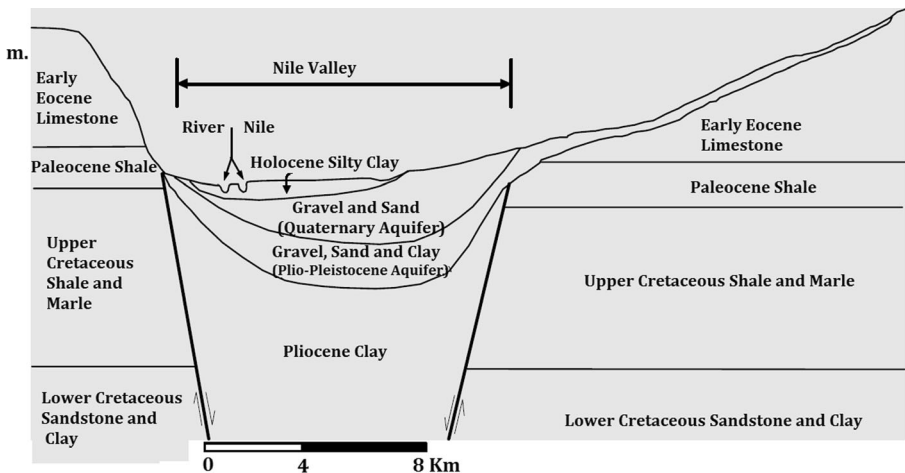


Fig. 4 Hydro-geologic cross section at Luxor area (After Ismail *et al.* 2006, p. 6)

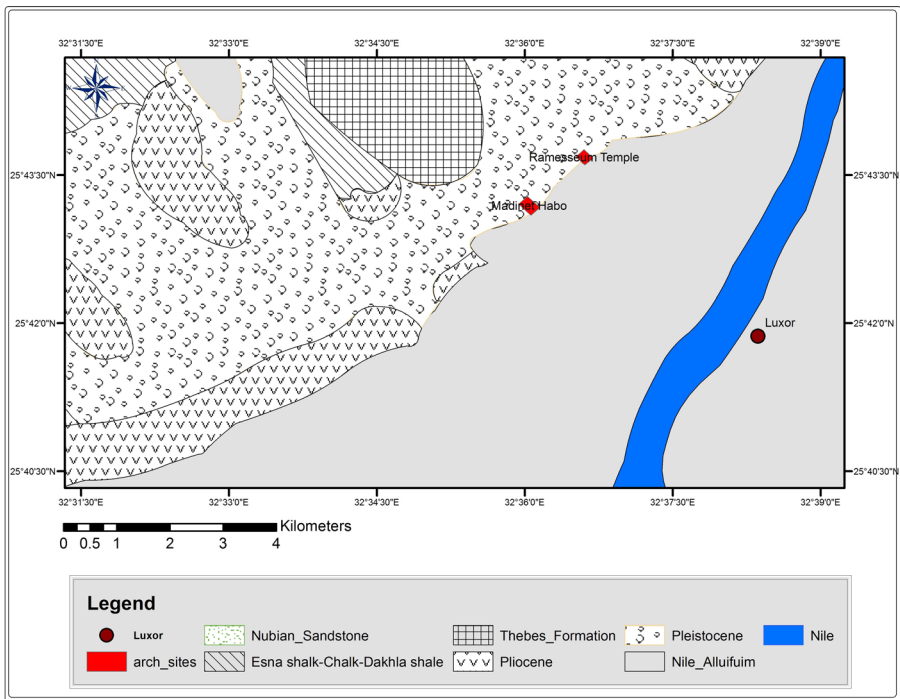


Fig. 5 Geological map around the archaeological area

represented by a Nile flood plain unit, attaining a total thickness of 18.5 m, made up of two sequential layers: silty clay and clay layers (Ahmed 2014) (Fig. 4).

From Esna to Luxor, the beds dip in a general northerly direction. In this area, a more complete section of lower Eocene rocks is exposed above the Esna shale. The Gebel Gurnah of Thebes, which lies on the western side of the Nile facing Luxor just behind the famous temple of Deir el-Bahari, commands a magnificent view of the Pharaonic monuments of that city. The section of this accessible hill is the type locality of the Thebes formation which is of lower Eocene age. This formation is about 290 m thick. It consists of limestone with many flint bands; these limestones overlie the Esna shale beds which measure about 55 m in thickness (Said 1962). Upper Egypt, from Luxor to Aswan, is characterized by a string of ancient Nubian sandstone quarries and two key quarry landscapes: Gebel el-Silsila (sandstone) and the Aswan area (granite, silicified sandstone, and sandstone) (Storemyr *et al.* 2007) (Fig. 5).

Environmental Risks

The Theban Necropolis is located in a dry desert, where the fertile Nile flood plain meets the arid Western Desert. Just beyond this border between growth and barrenness is the archaeological site. Limestone and silicified sandstone were the main building stones of ancient Egypt in the new Kingdom (Harrell and Storemyr 2009; Elwaseif *et al.* 2012). The first architects of the New Kingdom had no means of knowing the rock types

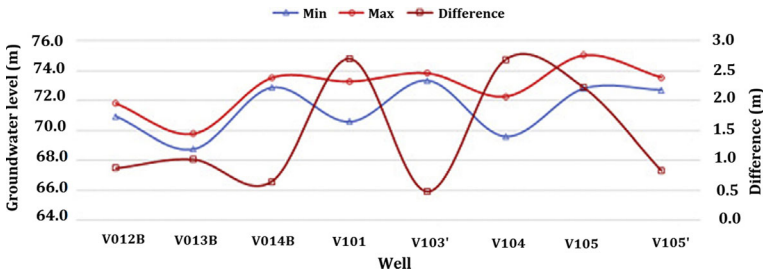


Fig. 6 The disparity of groundwater levels at Luxor area (after Ahmed and Fogg 2014, p. 100)

and associated structural complexity that might be encountered as the excavation proceeded (Aubry *et al.* 2011). The systematic use of Nubian sandstone as building material is found mainly in the construction of sandstone temples, such as the funeral temples at Qurna (except for parts of the Hatshepsut temple) (Klemm and Klemm 2002). Disintegration of Thebes limestones from Luxor due to humidity changes, and hence salt efflorescence, occurred within a few weeks, after relocating the rock samples to humid environments (Wüst and McLane 2000). Water rising by capillary action in the pore space between stone foundations vertically and horizontally may cause deterioration as far as the sub-soil water table is very close to the surface. The water level is the main factor eroding the temple foundation; for example, the residential area surrounding the project area has no house connections or sewerage system (El Qurna village) and they use holding tanks to allow wastewater to infiltrate into the subsurface water which will be moved out continuously through the proposed system. Stagnant water and wet wells are good media

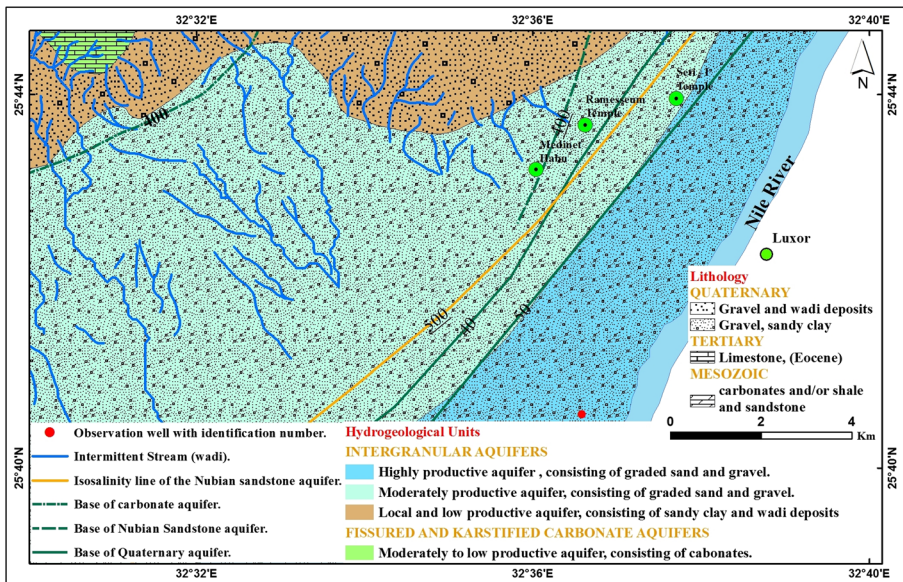
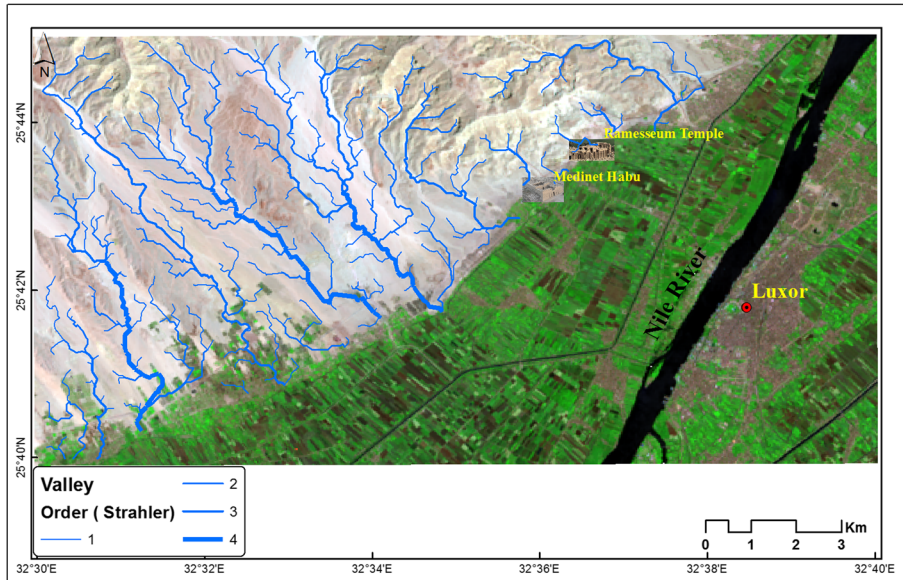
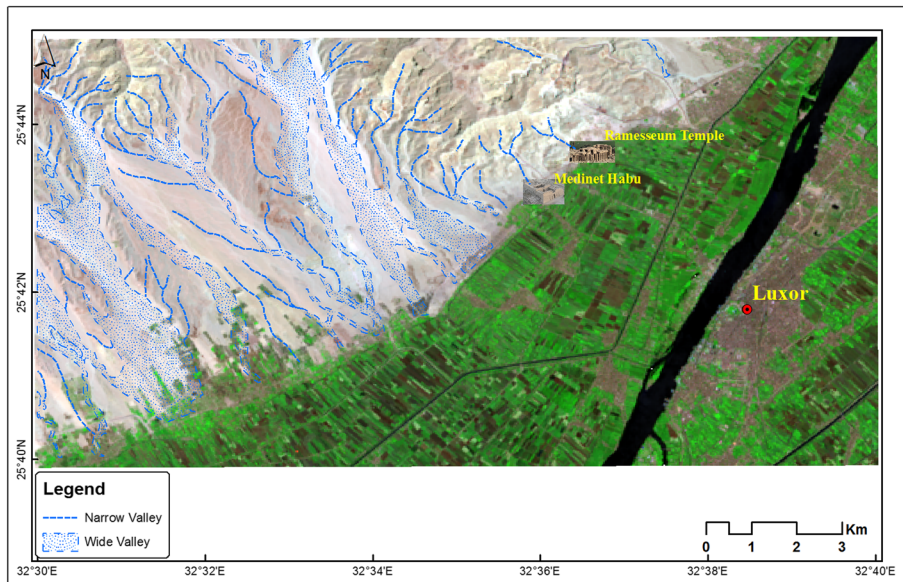


Fig. 7 Hydrogeological map of the study area



a



b

Fig. 8 The main valleys and the streams to detect the hydrogeological status around the study area by SRTM (a) and topographic map (b)

for fungi and algae growth and therefore re-potential for health risk (Figs. 6, 7, and 8a, b). Lowering the water table will reduce the health risk from water-related diseases (Figs. 9 and 10) (Zaghloul *et al.* 2008).



Fig. 9 The archaeological deteriorations as a result of the environmental risks (a–c) (Ramesseum temple)

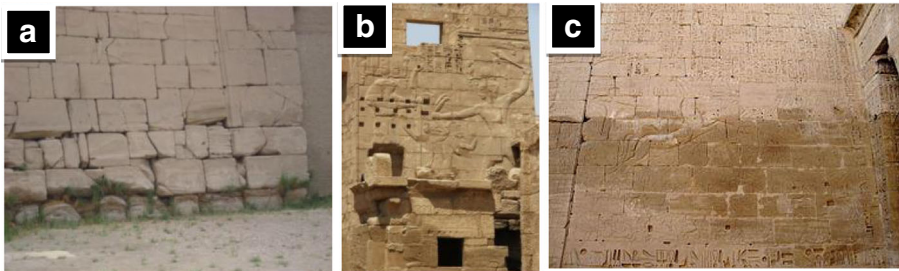


Fig. 10 The archaeological deteriorations as a result of the environmental risks (a–c) (Medinet Habu)

Material and Methodology

Materials

The present study involves the collection of topographic sheets 1:50,000 from Survey of Egypt. Geological and hydrogeological sheet was collected from national authority for remote sensing and space science. The required satellite imagery for the study area is to be downloaded from the USGS Earth Explorer (SRTM, ASTER, Coronaj-3 1970, Landsat TM 1984, Landsat ETM+ 2003, and L8 2016), and high-resolution data provided by national authority for remote sensing and space science (Spot4 2011 and Quickbird 2005) (Table 1). The ground truth data were in the form of reference data points collected using the Global Positioning

Table 1 Main satellite image properties

Number	Satellite	Sensor	Spatial resolution (m)	Acquisition date	Source
1	Corona j-3	KH-4B	1.8 m	20/08/1970	USGS
2	Landsat	TM	30 m	13/09/1984	GLCF
3	Landsat	ETM+	30 m	08/09/2003	GLCF
4	Quickbird	XS/P	0,6 m	24/11/2005	NARSS
5	Spot	4	10 m	18/04/2011	NARSS
6	Landsat	L8	30 m	30/08/2016	USGS

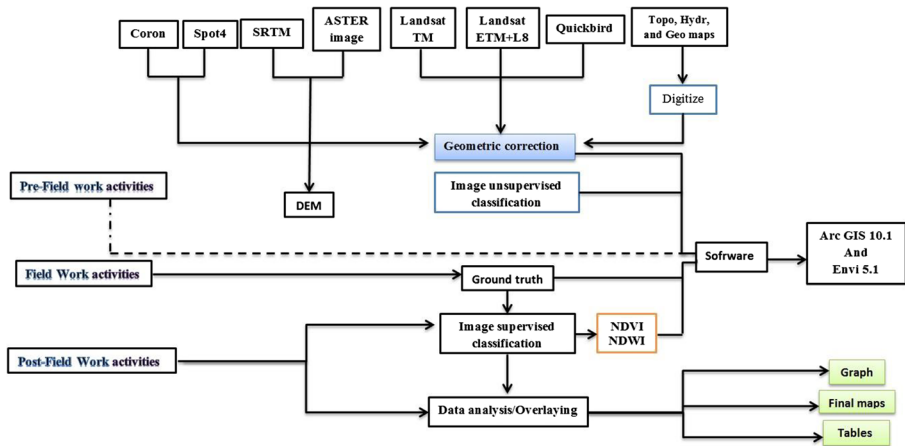


Fig. 11 Flowchart of the materials and methods

System (GPS). Map processing and image interpretation are done in ArcGIS 10.1 and ENVI 5.1 software. The obtained images are studied and analyzed to detect the changes in the layers based on past and present data. Prediction of future situation is done based on past data. Up-to-date maps are based on geological and topographic maps. Environmental modeling is based on topographic map layers by ArcGIS software (Fig. 11).

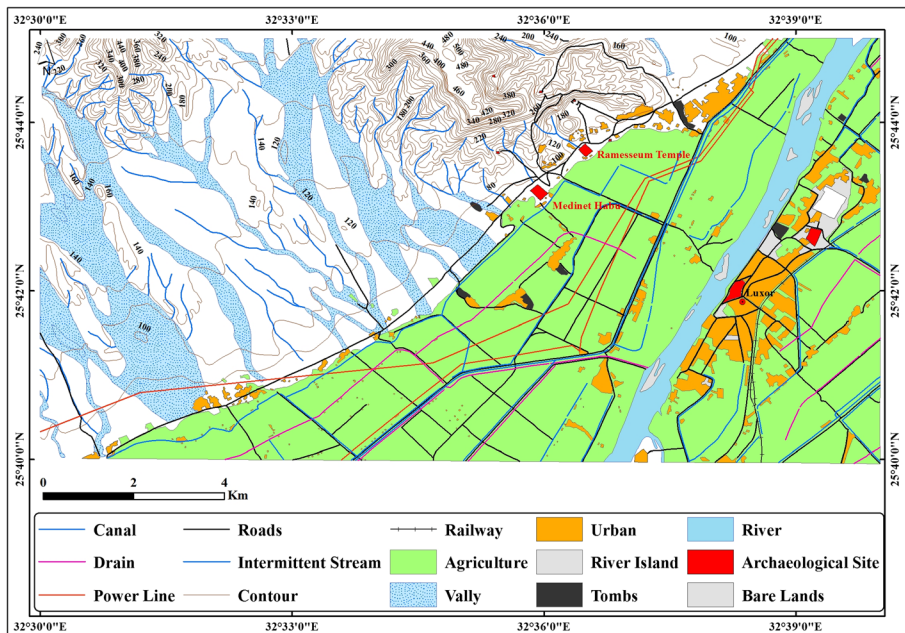


Fig. 12 Topographic map representing the various layers of the study area

Methodology

Image Preprocessing

– Geometric correction

The data were selected to be geometrically corrected, calibrated, and removed from their dropouts. These data were stratified into “zones,” where land cover types within a zone have similar spectral properties. Other image enhancement techniques like histogram equalization are also performed on each image for improving the quality of the image. The geometric correction of the data depended on topographic sheets of Egypt in the scale 1:50,000 with the spatial reference WGS_1984_UTM_zone_36N. Then accuracy assessment was carried out using 150 points from field data and existing land cover maps. To increase the accuracy of layer class, ancillary data and the result of visual interpretation were integrated with the classification result using GIS.

– Analysis in GIS

ArcGIS software (ArcMap 10.1) has been used to generate various thematic layers, like boundary, roads, railway network, and administrative boundary map using the topographic map (Fig. 12), geological map, and hydrogeological map. Digital maps of these classes are created by digitizing and processing boundaries between the layers by scanning photographs covering the area of interest and screen-digitizing their boundaries. These maps have to be geo-referenced and registered before they can be used in GIS analyses.

– Unsupervised classification of Images

Classification is based on measuring the reflection values in an image, depending on the local characteristics of the earth surface; in other words, there is a relationship between land cover and measured reflection values using many bands (multispectral classification). For the purposes of our investigations, an unsupervised classification method, based on the ISODATA clustering algorithm, has been herein used. The categorization has been done according to the number of classes required and the digital number of the pixels available. In particular, for Corona we used the panchromatic image (the only available satellite picture), whereas for all the other satellite dataset the spectral indices (computed as shown in formulas 1 and 2) have been used. The unsupervised classification has been used for reference and for understanding the statistical and spatial distribution of pixels with different digital numbers. Fourteen classes were used in the unsupervised classification for Corona, Quickbird, Spot, and Landsat TM, ETM+, and L8 images.

– Ground truth

During the field visits, a handheld GPS (Global Positioning System) was used to identify the exact position of the place under consideration with latitude and longitude and its type by visual observation. The ground truth data thus obtained was used to

verify the classification accuracy. The data of ground truth were adapted for each single classifier produced by its spectral signatures for producing series of classification maps.

– Supervised classification of images

In the supervised classification technique, the maximum likelihood algorithm was used. As for the unsupervised classification, for Corona we used the only available satellite picture, whereas for all the other satellite dataset the spectral indices were used (computed as shown in formulas 1 and 2). The categorization process is based on the use of training sets (signatures) provided by the user on the basis of field knowledge. The training data guide the software clusterization. In particular, five classes (urban, agriculture, water bodies, barren, and desert) have been used for all the satellite pictures processed and analyzed (Corona, Quickbird, Spot, and Landsat TM, ETM+, and L8 images). The classification gave the diverse layers for the diverse class present in the area under investigation. Two land cover classes, namely, agricultural land and urban area, have been identified in the study area and considered for the analyses, because they are the most meaningful for the purpose of our investigations.

Normalized Difference Vegetation Index The normalized difference vegetation index (NDVI) is a numerical indicator that uses the visible and near-infrared bands of the electromagnetic spectrum (Holme *et al.* 1987). It is adopted to analyze remote sensing measurements and assess whether the target being observed contains live green vegetation. This index is used in Landsat L8 2016 image to detect the vegetation value in the agriculture land around the study areas. The NDVI algorithm subtracts the red reflectance values from the near-infrared and divides it by the sum of near-infrared and red bands:

$$\left[NDVI = \frac{(NIR - RED)}{(NIR + RED)} \right] \quad (1)$$

Normalized Difference Water Index The Normalized Difference Water Index (NDWI) is a remote sensing derived index estimating the leaf water content at canopy level. Low NDWI values (in red) correspond to low vegetation water content and low vegetation fraction cover. In period of water stress, NDWI will decrease (Rokni *et al.* 2014). The equation has only two input variables: near-infrared (NIR) and short-wave infrared (SWIR) reflectance. The election of the NIR band is usually simple because the NIR band region (0.7–1 μm) is relatively narrow, and the NIR wavelength locations are very similar among different sensors. Conversely, the election of the SWIR band is more complicated because the SWIR region (1–3 μm) is much wider and some sensors provide two or more SWIR bands. This index is used in Landsat L8 2016 image to detect the vegetation value in the agriculture land around the study areas. The NDWI algorithm is

$$\left[NDWI = \frac{(NIR - SWIR)}{(NIR + SWIR)} \right] \quad (2)$$

Table 2 Change detection results

Class	Area 1970 km ²	Change detection ± km ²	Area 1984 km ²	Change detection ± km ²	Area 2003 km ²	Change detection ± km ²	Area 2005 km ²	Change detection ± km ²	Area 2011 km ²	Change detection ± km ²	Area 2016 km ²
Urban	0.330	0.856	1.190	0.330	1.520	0.137	1.660	0.227	1.880	0.746	2.630
agriculture	10.380	0.417	10.790	-0.284	10.510	-0.209	10.300	-0.090	10.200	-0.779	9.430

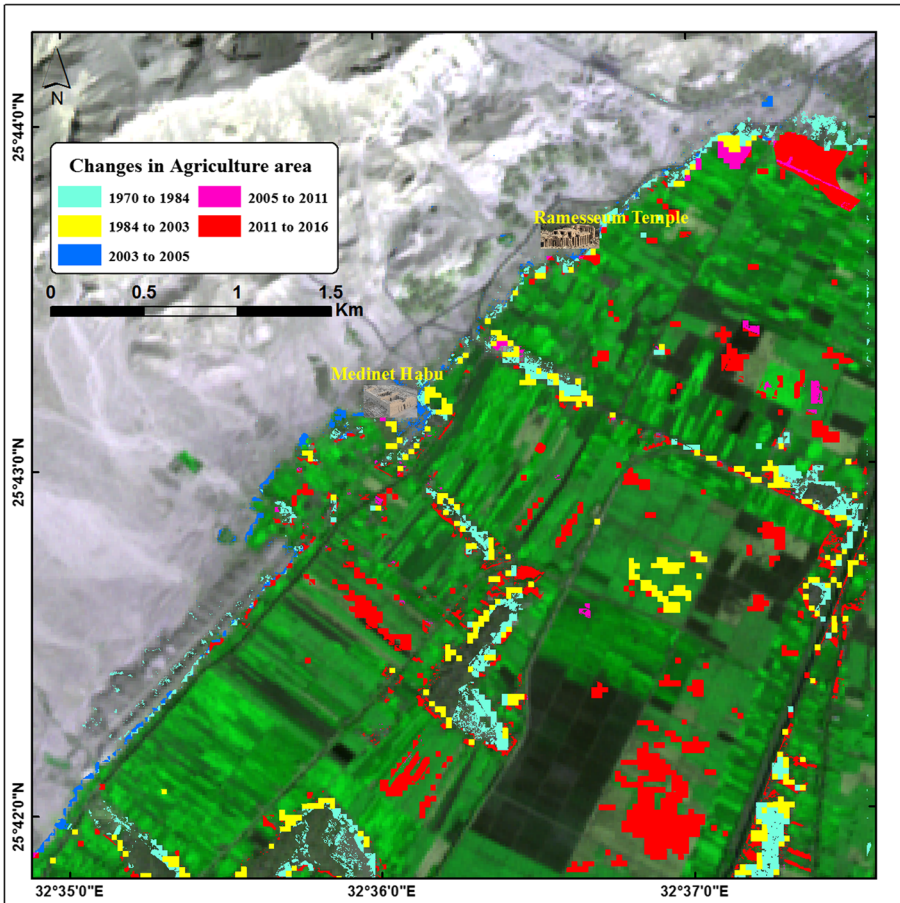


Fig. 13 The change rate in the agriculture lands between 1970 and 2016

Results

Change detection analysis described and quantified the differences between images of the same scene at different times. The acquisition dates (August, September, and November months) were mainly concerned to detect urban sprawl and changes in the vegetation value in the same agriculture season of the year. The classified images of the six dates were used to calculate the area of different land covers and observe the changes that are taking place in the span of data.

It is important to consider that our analysis has been focused on changes on two land cover classes: (i) agricultural land and (ii) urban area. In particular, the last one obviously did not depend on the season, but, considering the phenomenological behavior of the agricultural lands, we selected the cloud-free images most close to the same period of the year. The only exception was the SPOT image. Nevertheless, as highlighted in the following description and discussion of the classification results, we can argue that, as a whole, the change in agricultural lands is quite linear, and therefore, also in the case of SPOT image, the rate of the change is on the average (see Fig. 15). The different period of

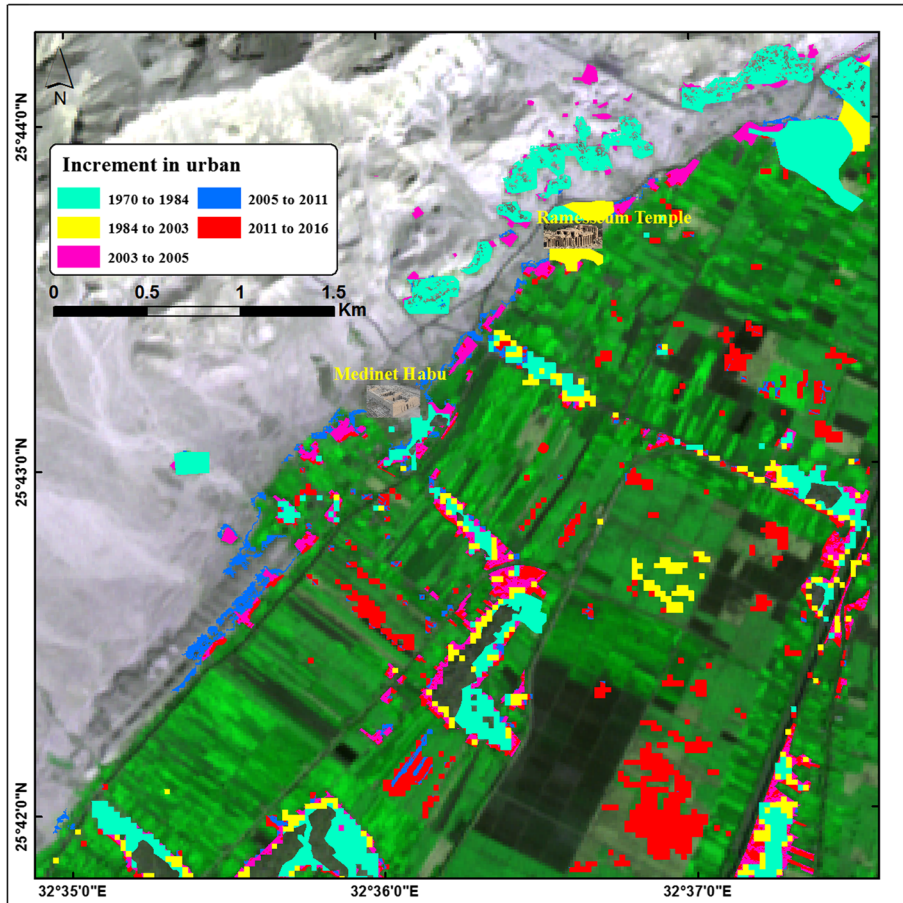


Fig. 14 The change rate in the urban lands between 1970 and 2016

the acquisition of the SPOT image does not have any (significant) impact. This is mainly due to the fact that the large part of the agriculture cultivation is made of banana tree (evergreen plant) and sugarcane; but in the last years, the banana cultivation is preferred by local farmers because it is much more convenient from the economical point of view.

In more detail, the analysis of Corona, Landsat, Spot, and Quickbird imagery revealed that agricultural lands were increased by about 0.417 km^2 from 1970 to 1984, but decreased about 0.284 km^2 from 1984 to 2003; in the same direction, the agriculture land decreased again by about 0.209 km^2 from 2003 to 2005. The agriculture land decreased also by about 0.090 km^2 from 2005 to 2011, and decreased again by about 0.779 km^2 from 2011 to 2016 (Table 2). On the other hand, we can see that the urban area was increased by about 0.856 km^2 from 1970 to 1984, in the same direction, the urban area was increased by about 0.330 km^2 from 1984 to 2003. The urban area increased also by about 0.137 km^2 from 2003 to 2005, and again the same area was increased by about 0.227 km^2 from 2005 to 2011; finally, the urban area increased by about 0.746 km^2 from 2011 to 2016 (Table 2). On the other hand, our investigations results showed that there was

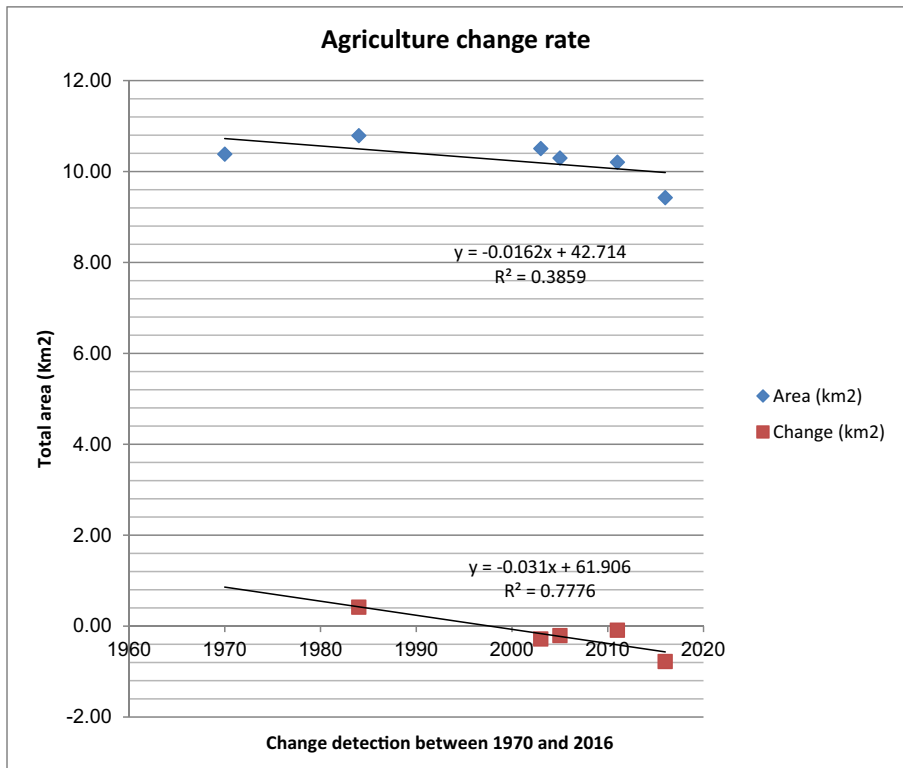


Fig. 15 Agriculture change rate graph

a decrease in the agriculture land space, also the study area has been affected by the high groundwater level (Fig. 13). As a whole, it was observed that the changes in the urban areas increased from 1970 to 2016 (Fig. 14). As a result of this situation, it was very clear that most of the environmental problems were caused by the effect of the agriculture lands (Fig. 15) and the urban sprawling around the study area (Fig. 16).

Discussion and Recommendation

Discussion

The use of remote sensing and GIS techniques in the archaeological field and cultural heritage management has a long history which started from the 1970s (Smith 2014). Remote sensing techniques are recognized to be a very important tool for monitoring desertification as well as land use and land cover changes, vegetation health and density, and landform processes (Chandra 2011). In this study, the detection of changes in urban and agricultural areas has been assessed from multitemporal and multisensor satellite images. In particular, the analysis of Corona, Landsat TM, Landsat ETM, Spot4, and Landsat L8 images was performed around a very important archaeological area (at the west side of Luxor) where the Medinet Habu and Ramesseum temples are located.

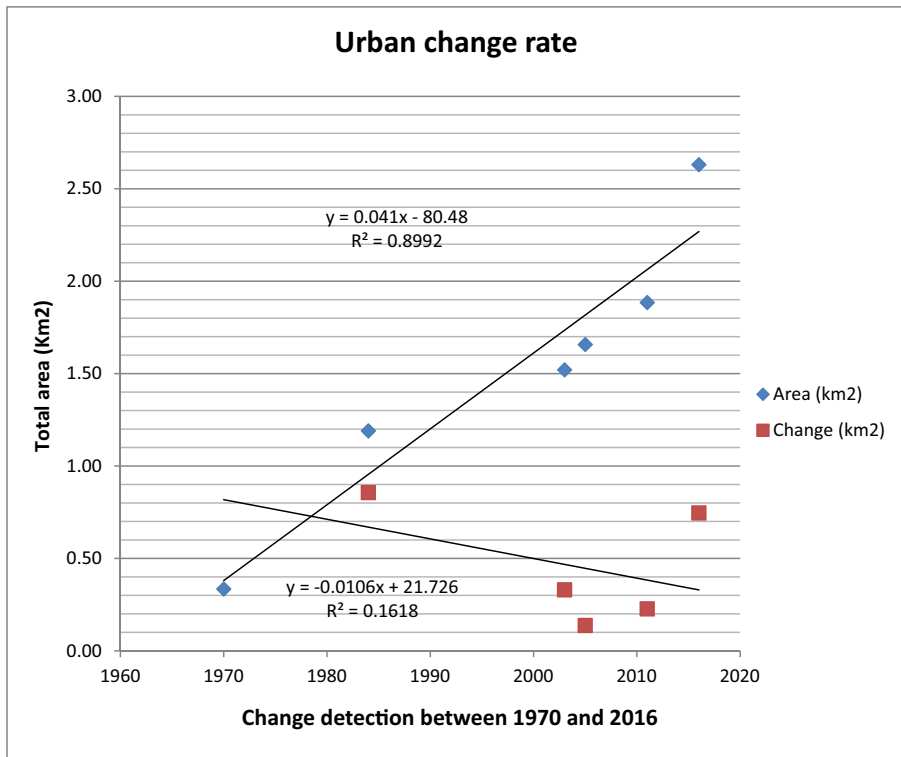


Fig. 16 Urban change rate graph

The results of the image processing revealed that the urban lands increased by about 37.28% from 1970 to 1984, about 14.37% from 1984 to 2003, about 5.96% from 2003 to 2005, about 9.88% from 2005 to 2011, and about 32.49% from 2011 to 2016. It was very clear that the increase in the urban sprawling at the west Luxor area has a continuous rate with high percentage between two periods 1970 to 1984, and 2011 to 2016. It was observed that the encroachment in the urban lands in west Luxor took place beside the two temples, also near the boundary of the desert. The groundwater level was monitored for six months. Piezometer readings were carried out from December 2005 to May 2006. Geophysical measurements suggest a strong connection, between increase in groundwater salinity and flowage towards the River Nile (Abraham and Bakr 2000). The tests have indicated the great depths of the groundwater and the high salinity content (Ahmed 2009). The average terrain elevation for the depth of the groundwater fluctuated about 4 m near Nile River and 2.5 m near Medinet Habu and Ramesseum temples. The “groundwater mound” forming under the ancient temples at Luxor appears as a result of the unplanned urban encroachment. Unfortunately, the archaeological area has been also affected by the agricultural encroachment near the temples as well as by the construction of the High Dam which further increased the water level in the Nile River. Due to the rising groundwater levels and soil salinity, some deterioration of monuments has been observed. The high values in the NDVI and NDWI indices evidence that there is high level in the groundwater and also high amount of water used for irrigation around the two temples. The antiquities here are threatened by the increase in salinity of the

groundwater contacting their foundations: “A top layer of silty clay, extending to a depth of 9 m below the ground surface, a layer of sand, between 9 and 14 m beneath the ground surface and layers of very stiff to hard silty clay, from 14 to at least 20 m (end of borings) beneath the surface” (Campos 2009). As the water evaporates, the salts crystallize, causing rapid decay of the rock of which these temples, statues, and tombs are constructed. The distribution in the levels of groundwater and temperature were the main reason in the deterioration of the Medinet Habu and Ramesseum temple. The degree of weathering damage appears to be much more dependent on exposure characteristics of the investigation areas and the local environmental conditions, especially as related to salt weathering processes. Some of the proposed solutions have been suggested using the remote sensing and GIS techniques to mitigate the risks of the groundwater.

Recommendations

An engineering system can be used as an effective method for groundwater lowering in the study area. According to Abdel-Warith (2007), cutoff walls (in the suggested boundary line 1) can be excavated using diaphragm wall equipment and filled with plastic concrete. This cutoff wall is to prevent groundwater from entering the soil below the monument. In order to control surface water, a system of horizontal drains (in the suggested boundary line 2 (Fig. 17a)) should be installed at the intended final groundwater level with sloping from the west to the east (Fig. 17b), and covered with a steel screen. Horizontal perforated pipes can discharge water to corner sumps in the east side,

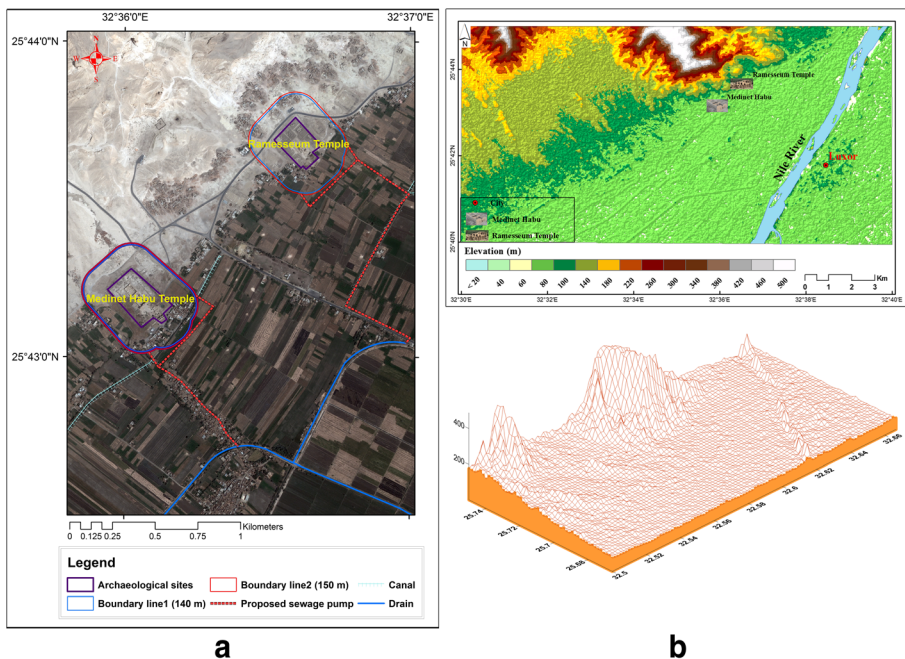


Fig. 17 Suggested solutions for groundwater lowering by Quickbird 2005 (composite RGB) (a) and digital elevation model “DEM” and 3D wireframe for the study area (b)

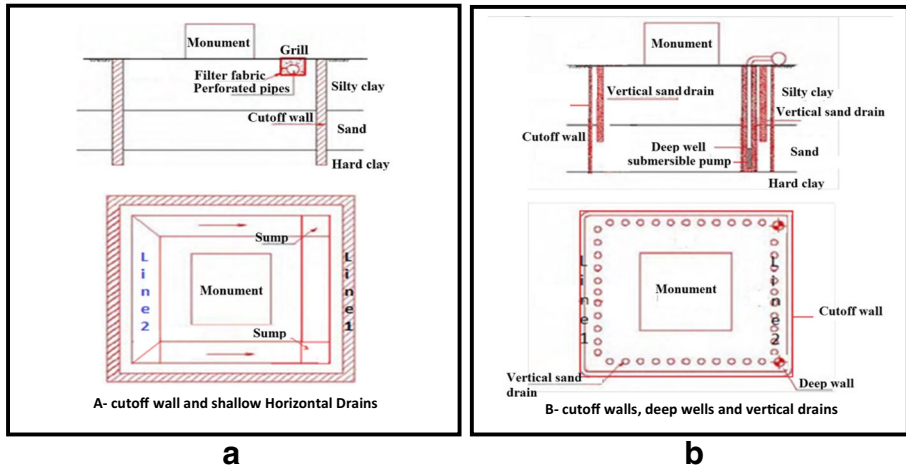


Fig. 18 Suggested solutions for groundwater lowering (a, b) (modified after Abdel-Warith 2007, p. 9)

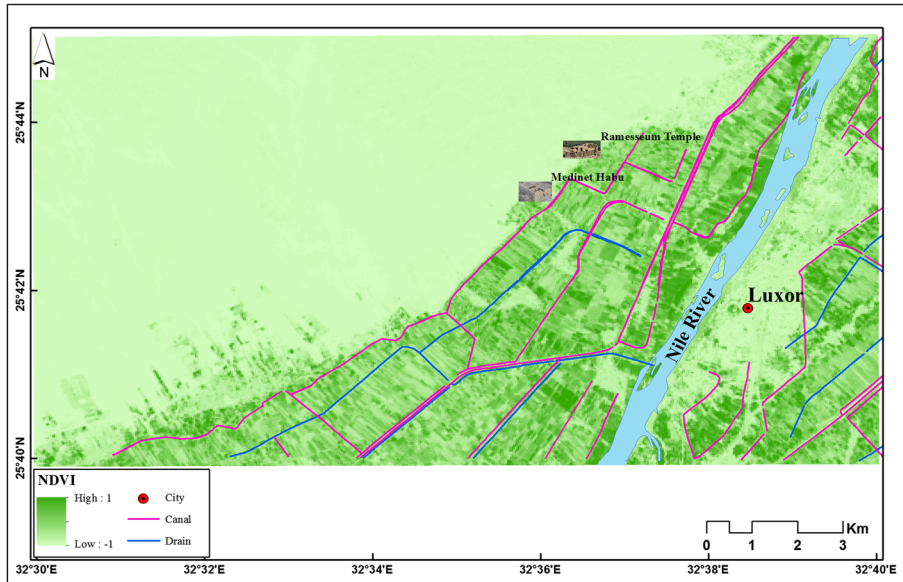
from which water can be pumped out of the site to the nearest drain and then to the nearest canal. The second method depends on the cutoff wall similar to the first example (in the suggested boundary line 1), in addition to deep wells that exist in the corners of the east side with submersible pumps to pump the groundwater from the sand aquifer to relieve the pressure on the bottom of the upper clay layer. While the suggested boundary line 2, to collect the groundwater, is designed with sloping from the west to the east. The submersible pumps in the deep wells in the east corners would be operated intermittently to keep the lowered groundwater level at the target elevation, with minimal influence on the monument. Discharge water can be sent to the nearest canal. This system would have a low construction cost (Fig. 18a, b).

- New irrigation techniques must be used instead of the ancient ones to avoid the groundwater level rising and dispensing on the crops like sugarcane and banana which need much water in irrigation with others which need too little quantity of water (Fig. 19a, b).

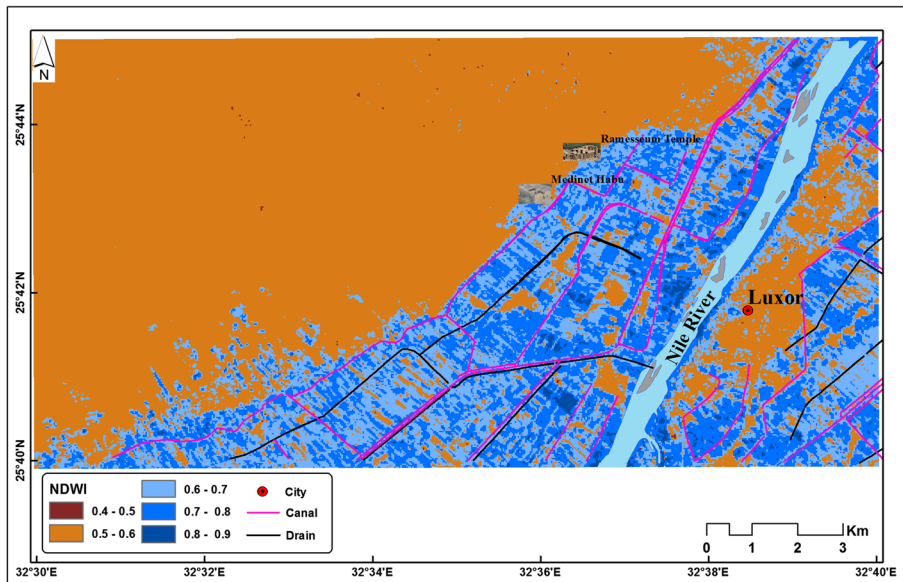
Conclusion

In this study, we used and operationally applied a multirate multisource satellite data set for investigating the environmental risks around Medinet Habu and Ramesseum temple. The analysis of multitemporal satellite data conducted into the GIS environment provided invaluable information about both the past asset of the area and its current conditions.

The joint analyses of the outputs from the diverse disciplines along with *in situ* investigations provided a comprehensive overview of the current environmental conditions and their interrelationships with human activities. The integrated analysis of results from satellite-based investigations with archaeological, geological, and hydrological studies suggested innovative solutions for risk mitigation strategies.



a



b

Fig. 19 The high amount of water absorption by the crops around the archaeological temples explained by “NDVI” (a) and “NDWI” in Landsat L8 2016 image (b)

In particular, the ongoing environmental changes and their negative impacts on the ancient structures and temples could be mitigated by actions (as suggested in the “Recommendations” section) addressed to keep lower the level of groundwater, in order to minimize the impact of the water on the monuments.

As a whole, results from our integrated analyses pointed out that urban sprawling and agriculture extents caused the deterioration of the temples and the previous environmental risks can be identified “as the main reason” that causes the monument deterioration. GIS data integration and modeling were helpful in devising innovation solutions to set up in order to preserve and protect the invaluable ancient temples and the structures present in the study area.

Among the key outcomes, our analysis highlights that satellite-based data integrated with *in situ* analysis and ancillary information have significant potential for operational applications, supporting the following:

1. The design of strategies of modern infrastructures and building
2. The integration between remote sensing with *in situ* analysis and ancillary information elaborated using GIS techniques and modeling was helpful in creating innovation solutions to protect the study area.

Acknowledgments These results are part of the PhD thesis of Mr. Abdelaziz Elfadaly. The authors would like to express their appreciation to the National Authority for Remote Sensing & Space Sciences (NARSS) for funding the PhD data. Thanks are given to the Institute of Methodologies for Environmental Analysis (CNR) for the support and for funding the publication. Thanks are also given to the Egyptian Cultural Affairs sector and the missions (Ministry of Higher Education) for funding the PhD study at Basilicata University.

References

- Abdel-Warith, A. (2007). Egypt infrastructure improvements project secondary cities scoping statement for city of Luxor groundwater lowering of antiquities sites on the west bank, (NOPWASD) and (USAID), p. 4.
- Abraham, G., & Bakr, A. (2000). Comprehensive development plan for the city of Luxor Egypt—Investment Project # 4, investment portfolio for the development of infrastructure serving New Luxor and El Toad, pp. 1–125.
- Agapiou, A., Hadjimitsis, D. G., Papoutsas, C., Alexakis, D. D., & Papadavid, G. (2011). The importance of accounting for atmospheric effects in the application of NDVI and interpretation of satellite imagery supporting archaeological research: the case studies of Palaepaphos and Nea Paphos sites in Cyprus. *Journal of Remote Sensing*, 3, 2605–2629.
- Ahmed, A. A. (2009). Land use change and deterioration of Pharaonic monuments in Upper Egypt. *Journal of Engineering Sciences, Assiut University*, 37(1), 161–177.
- Ahmed, A. A. (2014). Fluoride in quaternary groundwater aquifer, Nile Valley, Luxor, Egypt, Saudi Society for Geosciences 2013. *Arabian Journal of Geosciences*, 3073. doi:10.1007/s12517-013-0962-x
- Ahmed, A. A., & Fogg, G. E. (2014). The impact of groundwater and agricultural expansion on the archaeological sites at Luxor, Egypt. *Journal of African Earth Sciences*, 95, 100. doi:10.1016/j.jafears.2014.02.007
- Alexakis, D. D., Agapiou, A., Hadjimitsis, D. G., & Sarris, A. (2012). Remote sensing applications in archaeological research, isbn: 978-953-51-0651-7, Intech, available from: <http://www.intechopen.com/books/remote-sensingapplications/remote-sensing-applications-in-archaeology>, p. 435.
- Aubry, M., Berggren, W. A., Dupuis, C., Ghaly, H., Ward, D., King, C., Knox, R. W.O'B., Ouda, K., Youssef, M., & Galal, W. F. (2011). Pharaonic necrostratigraphy: a review of geological and archaeological studies in the Theban Necropolis, Luxor, West Bank, Egypt. *Terra Nova*, 21(4), 237–256, Blackwell Publishing Ltd, p. 23.
- Bednarski (2005). Holding Egypt: tracing the reception of the description de l'Égypte in nineteenth-century, Great Britain Golden House Publications, Printed in the United Kingdom London, p. 87.

- Bennett, R. (2011). Archaeological remote sensing: visualisation and analysis of grass-dominated environments using airborne laser scanning and digital spectra data, Dissertation submitted in partial fulfilment of the requirements for the degree 'Doctor of Philosophy', awarded by Bournemouth University, p. 10.
- Blackman, A. M. (1923). Luxor & its temples, Printed in Great Britain Billing and Sons, Ltd., Guildford and Eshek, pp. 120–160.
- Butt, A., Shabbir, R., Ahmad, S., & Aziz, N. (2015). Land use change mapping and analysis using remote sensing and GIS: a case study of Simly watershed, Islamabad, Pakistan. *The Egyptian Journal of Remote Sensing and Space Science*, 18(2), 252.
- Campos, E. (2009). A groundwater flow model for water related damages on historic monuments—case study West Luxor Egypt. *Vatten*, 65, 247–254.
- Casciati, S., & Borja, R. I. (2004). Dynamic FE analysis of south Memnon colossus including 3D soil–foundation–structure interaction. *Computers and Structures*, 82(2004) 1719–1736), 1721.
- Challis, K. and Andy Howard, J. 2006. A Review of trends within archaeological remote sensing in alluvial environments, Published online 13 November 2006 in Wiley inter Science (www.interscience.wiley.com). doi:10.1002/arp.296. p. 1.
- Chandra, P. (2011). Performance evaluation of vegetation indices using remotely sensed data. *International Journal of Geomatics and Geosciences*, 2(1), 231–240.
- Cigna, F., Lasaponara, R., Masini, N., Milillo, P., & Tapete, D. (2014). Persistent scatterer interferometry processing of COSMO-SkyMed StripMap HIMAGE time series to depict deformation of the historic centre of Rome, Italy. *Remote Sensing*, 6(12), 12593–12618.
- Corrie, R. (2011). Detection of ancient Egyptian archaeological sites using satellite remote sensing and digital image processing, Earth Resources and Environmental Remote Sensing/GIS Applications II, edited by Ulrich Michel, Daniel L. Civco, Proc. of SPIE Vol. 8181, 81811B, 2011 SPIE, p. 1.
- Elwaseif, M., Ismail, A., Abdalla, M., Abdel-Rahman, M., & Hafez, M. (2012). A 2012 geophysical and hydrological investigations at the west bank of Nile River (Luxor, Egypt). *Environment and Earth Science*, 67, 911–921. doi:10.1007/s12665-012-1525-2.
- Fisher, M. M. (2009). The eighteenth dynasty temple, part 1 “the inner sanctuaries”. *The university of Chicago Oriental Institute Publications*, 136, 1–89.
- Harrell, J.A., and Storemyr P 2009 Ancient Egyptian quarries—an illustrated overview. In N. Abu-Jaber, E.G. Bloxam, P. Degryse, & T. Haldal (Eds.), *Quarry scopes: ancient stone quarry landscapes in the Eastern Mediterranean* (pp. 8–9). Geological Survey of Norway Special Publication, 12.
- Holme, A., Burnside, D., & Mitchell, A. (1987). The development of a system for monitoring trend in range condition in the arid shrublands of Western Australia. *Australian Rangeland Journal*, 9, 14–20.
- Holscher, U. (1941). *The mortuary temple of Ramses III part 1, translated by Mrs. Keith C. Seele* (pp. 1–134). U.S.A: The University of Chicago Press.
- Ismail, A., Anderson, N. L., Rogers, J.D., Abbas, M. A., & Atekwana, E. A. (2006). Hydro geophysical Investigation at Luxor, Southern Egypt. <http://www.dot.state.fl.us/statematerialsoffice/geotechnical/conference/materials/ismailanderson-rogers-abbas-atekwana.pdf>, p. 6.
- Johnson, J. K. (2006). *Remote sensing in archaeology* (p. 130). Mississippi: The University of Alabama Press, Tuscaloos Published for The Center for Archaeological Research at the University of Mississippi.
- Kelong, T., Yuqing, W., Lin, Y., Riping, Z., Wei, C., & Yaobao, M. (2008). A new archaeological remote sensing technology, the International archives of the photogrammetry. *Remote Sensing and Spatial Information Sciences*, XXXVII(Part B7. Beijing 2008), 221.
- Khorrarn, S., Koch, F. H., van der Wiele, C. F., & Nelson, S. A. C. (2012). *Remote sensing, Library of Congress control number: 2012930489* (p. 76). Berlin (www.springer.com): Springer Science+Business Media.
- Klemm, D. D., & Klemm, R. (2002). The building stones of ancient Egypt—a gift of its geology. *Journal of African Earth Science*, Published by Elsevier Science Ltd, p. 637.
- Lasaponara, R., & Masini, N. (2012). *Satellite remote sensing (a new tool for archaeology)*, Library of Congress control number: 2011946224 (p. 162). Berlin (www.springer.com): Springer is part of Springer Science+Business Media.
- Lasaponara, R., & Masini, N. (2013a). Satellite synthetic aperture radar in archaeology and cultural landscape: an overview. *Archaeological Prospection*, 20(2), 71–78.
- Lasaponara, R., & Masini, N. (2013b). Full-waveform airborne laser scanning for the detection of medieval archaeological microtopographic relief. *Journal of Cultural Heritage*, 10, e78–e82.
- Lasaponara, R., Masini, N., Rizzo, E., & Orefici, G. (2011). New discoveries in the Piramide Naranjada in Cahuachi (Peru) using satellite, ground probing radar and magnetic investigations. *Journal of Archaeological Science*, 38(9), 2031–2039.

- Lasaponara, R., Leucci, G., Masini, N., Persico, R., & Scardozzi, G. (2016). Towards an operative use of remote sensing for exploring the past using satellite data: the case study of Hierapolis (Turkey). *Remote Sensing of Environment*, 174, 148–164.
- Levin, N. (1999). Fundamentals of Remote Sensing, p. 8. <http://www.geoservis.ftn.uns.ac.rs/downloads/ISP/1999-fundamentals-of-remote-sensing.pdf>.
- Masini, N., & Lasaponara, R. (2006). Satellite-based recognition of landscape archaeological features related to ancient human transformation. *Journal of Geophysics and Engineering*, 3(3), 230.
- Masini, N., Lasaponara, R., & Orefici, G. (2009). Addressing the challenge of detecting archaeological adobe structures in Southern Peru using QuickBird imagery. *Journal of Cultural Heritage*, 10, e3–e9.
- McLane, J., Wüst, R. A. J., Porter, B., & Rutherford, J. (2003). Flash-flood impacts and protection measures in the Valley of the Kings, Luxor, Egypt. *APT Bulletin*, 34(1), 37–45.
- Mosbeh, I. R. H., & Kaloop, R. (2015). Monitoring urban growth and land use change detection with GIS and remote sensing techniques in Daqahlia governorate Egypt, Gulf Organisation for Research and Development. *International Journal of Sustainable Built Environment, International Journal of Sustainable Built Environment*, 4, 117–124(2015), 118.
- Murray, M. A. (2002). Egyptian temples, London Sampson low, Marston6 Co., LTD, printed in Great Britain by Purnell and Sons, pp. 132–158.
- Orlando, P., & Villa, B. (2011). Remote sensing applications in archaeology. *Archeologia e Calcolatori*, 22(2011), 147–168.
- Parcak, S. H. (2009). Satellite remote sensing for archaeology, First published 2009 by Routledge 2 Park Square, Milton Park, Abingdon, Oxon OX14 4RN Simultaneously published in the USA and Canada by Routledge 270 Madison Ave., New York, NY 10016, p. 38.
- Peters, S. M. (2011) Decoding the Medinet Habu inscriptions: the ideological subtext of Ramesses III's war accounts, word count: 17,070 (with footnotes + bibliography included), pp. 1–55.
- Quibell, J. E. (1898) The Ramesseum, London: printed by William Clowes and Sons, Limited, Stamford Street and Charing Cross 1898, pp. 1–20.
- Rajan, Y. S., & Ninan, J. (1983). International scene in remote sensing. *Proceedings of Indian Academy of Sciences (Engineering Science)*, 6(4), 355–371.9 Printed in India, p. 357.
- Rokni, K., Ahmad, A., Selamat, A., & Hazini, S. (2014). Water feature extraction and change detection using multitemporal Landsat imagery. *Journal of Remote Sensing*. (www.mdpi.com/journal/remotesensing). pp. 4173–4189.
- Roudgarni, P., Monavari, M., Fegghi, J., Nouri, J., & Khorasani, N. (2008). Environmental impact prediction using remote sensing images. *Journal of Zhejiang University SCIENCE A* ISSN 1673-565X (Print); ISSN 1862-1775 (Online). www.zju.edu.cn/jzus/; www.springerlink.com. p. 381.
- Said, R. (1962) The geology of Egypt, PH. D. (Harvard) Cairo University, Gizeh (Egypt, U.A.R.), Elsevier publishing company Amsterdam-New York, Library of Congress Catalog Card Number 61-18143, pp. 93.
- Skidmore, A. (2003). Environmental modeling with GIS and remote sensing, published In the USA and Canada, second publishing, p. 8.
- Smith, C. (2014). Encyclopedia of Global Archaeology. doi:10.1007/978-1-4419-0465-2, New York, pp. 3631–4147.
- Storemyr, P., Bloxam, E., Adel Kelany, T. H., Harrell, J. A., Youstri, R., & Fathy, E. (2007). Risk assessment and monitoring of ancient Egyptian quarry landscapes, Printed at the Geological Survey of Norway, p. 103.
- Tapete, D., Cigna, F., Masini, N., & Lasaponara, R. (2013). Prospection and monitoring of the archaeological heritage of Nasca, Peru, with ENVISAT ASAR. *Archaeological Prospection*, 20(2), 133–147.
- Virginia L. E. (2011). Mud-brick architecture. In Willeke Wendrich (ed.), *UCLA Encyclopedia of Egyptology*, Los Angeles. <http://digital2.library.ucla.edu/viewItem.do?ark=21198/zz0026w9hb>, pp. 1–9.
- Wiseman, J., & El-Baz, F. (2007). *Remote sensing in archaeology, Library of Congress control number: 2001012345* (p. 71). Berlin: Springer Science.
- Wüst, R. A. J., & McLane, J. (2000). *Rock deterioration in the Royal Tomb of Seti I* (p. 184). Egypt: Elsevier Science B.V. www.elsevier.nl/locate/enggeo, All rights reserved.
- Zaghloul, E.A., El-Dessouki, A., Hawwas, Z., Fayed, A., Elbeih, S., El-Nawawy, I., Meikhaeil, N., Bahy El-Din, A., & Ragi, I. (2008). Using remote sensing and GIS techniques to monitor the geo-environmental changes around Madinat Habo, west Luxor, Egypt.

Further reading

<http://glcfapp.glcf.umd.edu/Luxor>.
<http://edcns17.cr.usgs.gov/EarthExplorer/>.